



Land use and climate change effects on soil organic carbon in North and Northeast China

Yin Zhou^{a,b}, Alfred E. Hartemink^b, Zhou Shi^{a,c,d,*}, Zongzheng Liang^a, Yanli Lu^e

^a Institute of Agricultural Remote Sensing and Information Technology Application, Zhejiang University, Hangzhou, 310058, China

^b University of Wisconsin-Madison, Department of Soil Science, FD Hole Soils lab, 1525 Observatory Drive, Madison 53706, USA

^c Key Laboratory of Spectroscopy Sensing, Ministry of Agriculture, Hangzhou, China

^d State Key Laboratory of Soil and Sustainable Agriculture, Institute of Soil Science, Chinese Academy of Sciences, Nanjing, China

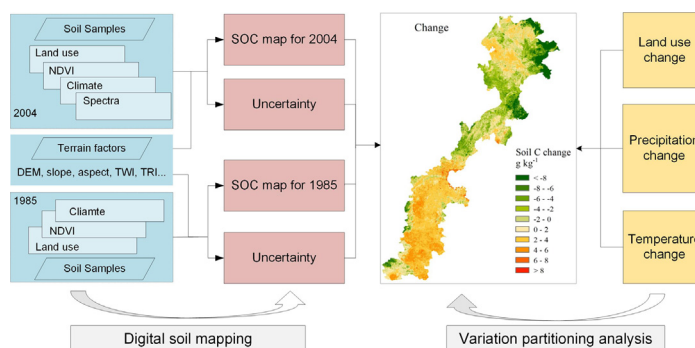
^e Institute of Agricultural Resources and Regional Planning, Chinese Academy of Agricultural Sciences, Beijing 100081, China



HIGHLIGHTS

- Digital soil mapping was efficient for evaluation of the SOC changes at large scale with limited data.
- Topsoil organic carbon increased in North China and rapidly decreased in Northeast China, however its stock remained neutral.
- Land use is the predominant driving factor of the SOC changes in North and Northeast China.

GRAPHICAL ABSTRACT



ARTICLE INFO

Article history:

Received 16 May 2018

Received in revised form 1 August 2018

Accepted 2 August 2018

Available online 04 August 2018

Editor: Jay Gan

Keywords:

Digital soil mapping

Soil carbon change

Land use change

Climate change

ABSTRACT

Soil is recognized as the largest carbon reservoir in the terrestrial ecosystem. Soil organic carbon (SOC) is vulnerable to changes in land use and climate. For a better understanding of the SOC dynamics and its driving factors, we collected data of the 1980s and 2000s in the North and Northeast China and conducted the digital soil mapping for spatial variation of SOC for the respective period. In the 1980s, 585 soils were sampled and the area was resampled in 2003 and 2004 (1062 samples) in a 30-km grid. The main land use in the area was cropland, forest and grassland. The random forest was used to predict the SOC concentration and its temporal change using land use, terrain factors, vegetation index, vis-NIR spectra and climate factors as predictors. The average SOC concentration in 1985 was 10.0 g kg^{-1} compared to 12.5 g kg^{-1} in 2004. The SOC variation was similar over the two periods, and levels increased from south to north. The estimated SOC stock was 1.68 Pg in 1985 and 1.66 Pg in 2004, but the SOC changes were different under different land uses. Over the twenty-year period, average temperatures increased and large areas of forests and grassland were converted to cropland. SOC under cropland was increased by 0.094 Pg (+9%) whereas 0.089 Pg SOC was lost under forests (−25%) and 0.037 Pg in the soils under grassland (−25%). It is concluded that land use is the main drivers for SOC changes in this area while climate change had different contributions in different regions. SOC loss was remarkable under the land use conversion while cropland has considerable potential to sequester SOC.

© 2018 Elsevier B.V. All rights reserved.

* Corresponding author at: Institute of Agricultural Remote Sensing and Information Technology Application, Zhejiang University, Hangzhou 310058, China.
E-mail address: shizhou@zju.edu.cn (Z. Shi).

1. Introduction

The increase in atmospheric greenhouse gas (GHG) has steered attention on soil organic carbon (SOC) as soils contain the largest carbon stock of all terrestrial ecosystems. The balance between SOC inputs and outputs influences greenhouse gas and affects the global climate. Small changes in SOC stock impacts the carbon cycle and may significantly increase or decrease the carbon concentrations in the atmosphere. Soil carbon change is influenced by the climate and land use and varies in different soils. Changes in land use are the second source of GHG emissions to the atmosphere after fossil fuel burning (IPCC, 2013). The replacement of forest and natural grassland to cropland may cause a reduction of SOC (Don et al., 2011). In contrast, improved soil management in agriculture, such as conversion from cropland into grassland and afforested or longer fallow intervals, can reduce emissions by SOC sequestering since plant residues and roots are accumulated in the soil as soil organic matter (Guo and Gifford, 2002).

There have been a considerable number of studies on soil carbon mapping for a specific period across different scale (McBratney et al., 2003; Viscarra Rossel et al., 2014). Fewer studies have investigated SOC dynamics and changes over time. Some studies have estimated the effect of land use change on soil carbon through the use of long-term experiments (e.g. Costa Junior et al., 2013), or using process-based models such as CENTURY, SPEROS-C or RothC (Falloon and Smith, 2002; Nadeu et al., 2015). These models contain various parameters that represent the soil carbon cycle processes which can handle past or future scenarios. As these methods require data from long-term experiments, they are usually limited to small areas.

Digital soil mapping is an efficient method to examine the spatial variation of soil information with diverse auxiliary data and statistical techniques (McBratney et al., 2003; Sanchez et al., 2009). Digital mapping of SOC has been conducted by extraction the soil–environment relationship with covariates such as topography, vegetation indices, climate, land use, soil types (McBratney et al., 2003). Topography and soil types are relatively stable within decades while vegetation and land use are influenced by human activities (Grinand et al., 2017), as well as climate. Remote sensing technology can assess land use, climate and vegetation indices over time (Stow et al., 2004; Chen et al., 2018). Most digital soil C mapping studies have focused on the spatial assessment of SOC levels – few studies have investigated SOC changes over time across large areas.

In this study, we used historical SOC data with a range of environmental covariates in North and Northeast China. The objectives of the study were to map SOC in 1985 and 2004, assess the SOC changes over time, and identify SOC changes under different land use and climate change.

2. Materials and Methods

2.1. Study area

The area is located in the Northeast and Northern Plains, China, covering approximately 642 000 km². Cropland is the dominant land use. The southern part of the region, which belongs to the North China Plain, has a long history of agricultural development (Han et al., 2018). The North China Plain has a temperate monsoon climate, its mean annual precipitation ranges from 343 to 1277 mm yr⁻¹ and mean annual temperature ranges from 2 to 14 °C (Han et al., 2018). The northern part of the region has a shorter history of cultivation than the south part. Most parts of Northeast China belong to the temperate zone. The climate is cool and humid affected by the Eastern Asia Monsoon. The annual temperature ranges from 2.0 to 5.0 °C and annual precipitation ranges from 300 to 1000 mm yr⁻¹ (Ye et al., 2009).

2.2. SOC data

The historical data was from the Second National Soil Survey of China with an average year of 1985 (Shi et al., 2004). The survey provided detailed information on soil taxonomic classification, soil thickness, soil organic matter, bulk density, coarse fragments. A total of 585 soil samples were in the study area. The soil samples were collected by genetic horizons continuously down along the depth. As the depths of the horizons are inconsistent, an equal-area smoothing spline depth function as in Bishop et al. (1999) was used to calculate the 0–20 cm top SOC concentrations. For a given soil profile, the boundary of the horizons are denoted by x_i ($i = 0, 1, 2, \dots, n$), $x_0 < x_1 < x_2, \dots < x_n$ the soil property values y_i at specific i th layer, are modeled as:

$$y_i = \bar{f}_i + e_i \quad (1)$$

where \bar{f}_i is the mean value of soil property at depth between x_{i-1} and x_i , and e_i are measurement error with a mean of 0 and a variance of σ^2 . We denote $f(x)$ as the spline function of soil property at x depth, which can be found by minimizing:

$$\frac{1}{n} \sum_{i=1}^n (y_i - \bar{f}_i)^2 + \lambda \int_{x_0}^{x_n} [f'(x)]^2 dx \quad (2)$$

where the first term represents the fit of the spline to the data; the second term measures the roughness of the function $f(x)$. The λ parameter controls the trade-off between the fit and the roughness of the spline. Here we use a medium lambda value of 0.01 to obtain the 0–20 cm SOC concentration.

The area was resampled in 2003 and 2004 and 1062 samples from 0 to 20 cm soil depth were collected in a 30-km grid. The samples were air-dried and sieved to <2 mm. All samples were analyzed for soil organic matter colorimetrically after H₂SO₄ dichromate oxidation at 150 °C. Diffuse reflectance spectra of air-dried samples were measured using an ASD Fieldspec ProFR vis–NIR spectrometer with a spectral range of 350–2500 nm under laboratory condition. After removing the noise at 350–400 and 2451–2500 nm, the remaining spectra in the 400–2450 nm range were smoothed with a Savitzky–Golay filter (Shi et al., 2015). The spectra were transformed with a principal component analysis and the first three principal components (PC1, PC2 and PC3), accounted for 92%, 4% and 1% of the total variance respectively, were used.

The samples with SOM were converted to SOC by the relation between SOM and SOC using van Bemmelen factor:

$$\text{SOC} = \text{SOM}/1.724 \quad (3)$$

2.3. Environmental covariates

Environmental covariates used in this study included remotely sensed data, digital elevation model (DEM) and proximal sensing data (Table 1). Several types of remote sensing data were used, including, Moderate Resolution Imaging Spectroradiometer (MODIS), The Global Inventory Modeling and Mapping Studies (GIMMS), Tropical Rainfall Measuring Mission (TRMM) and Shuttle Radar Topographic Mission (SRTM).

MODIS is useful in land surface research and provides information on basic surface information. GIMMS is a NDVI product available from 1981 to 2006 and the data were obtained from Advance Very High Resolution Radiometer (Tucker et al., 2004). The intra-annual variance of the NDVI (VNDVI) was computed as an indicator for land cover variations since its temporal change is linked to the state of the surface vegetation (Zhou et al., 2016). The third type of remotely sensed data for precipitation used in this study was TRMM, and in particular, products

Table 1
Environmental covariates used in the prediction models for 1985 and 2004.

Environmental variables	SCORPAN factor	Data origin		Resolution		Reference
		1985	2004	1985	2004	
Land use	soil	RESDC	RESDC	1 km	1 km	Liu et al. (2014)
Soil spectra (PC1, PC2, PC3)	soil		ASD Fieldspec ProFR			
NDVI	vegetation	GIMMS	MODIS	8 km	250 km	NASA LP DAAC (2001) Tucker et al. (2004)
VNDVI	vegetation	GIMMS	MODIS	8 km	250 km	NASA LP DAAC (2001) Tucker et al. (2004) Ma et al. (2017)
Precipitation (mm)	climate	meteorological stations	TRMM		0.25°	
Temperature (°C)	climate	meteorological stations	meteorological stations			
Elevation (Ele, m)	terrain	SRTM	SRTM	1 km	1 km	USGS (2006)
Slope (°)	terrain	SRTM	SRTM	1 km	1 km	USGS (2006)
Curvature	terrain	SRTM	SRTM	1 km	1 km	USGS (2006)
Aspect (°)	terrain	SRTM	SRTM	1 km	1 km	USGS (2006)
MBI	terrain	SRTM	SRTM	1 km	1 km	USGS (2006)
TRI	terrain	SRTM	SRTM	1 km	1 km	USGS (2006)
TWI	terrain	SRTM	SRTM	1 km	1 km	USGS (2006)

of 3B42 (Ma et al., 2017). The annual values for 2004 and 1985 of the remote sensing data were calculated.

Digital elevation model provides terrain information, and it was derived from the 90-m SRTM data. Terrain attributes, including slope, curvature, mass balance index (MBI), terrain ruggedness index (TRI) and topographic wetness index (TWI) were derived from the DEM using SAGA GIS (<http://www.saga-gis.org>).

We used ground observations provided by the Chinese Meteorological Data Sharing Service System (<http://cdc.nmic.cn>). There are 105 meteorological stations across our study area that collect daily precipitation and temperature. The annual precipitation and temperature of 1985 and 2004 were calculated and interpolated to the whole study area by inverse distance weighting.

We obtained land use data from the Data Center for Resources and Environmental Sciences, Chinese Academy of Sciences (RESDC) (<http://www.resdc.cn>) for late 1980s and 2005.

The proximal sensed spectra measured of the soil samples in 2003 and 2004 were interpolated onto the whole study area using inverse distance weighting in ArcGIS 10.0.

2.4. Mapping the soil organic carbon and its uncertainty

Random forest (RF) was used to model the relationships between the SOC and the environmental covariates. The RF model is based on classification and regression trees (CART) methodology. To guarantee the model stability, RF grows a series of trees which benefits from random subsets of original training data sampling to build each tree (Breiman, 2001). Only a randomly chosen subset of predictors is used to produce the best split. The number of trees was set to 500. The prediction for regressions is the average of all tree results, while it is the majority of the correct classified outputs for classifications. The RF algorithm estimates the predictor importance by measuring the mean decrease in prediction accuracy.

We used bootstrap which is a non-parametric statistical technique for estimating the uncertainties of SOC predictions. Random errors are generated from the samples and predictors, and we resampled each model and the predictors creating a set of SOC probability distributions through performing the individual model of bootstrap samples. The final SOC predictions were an average of the bootstrapped models. The uncertainty was quantified by the confidence interval (CI) at 95% level, and each of the pixels was assigning to derive the CI. The uncertainty was expressed as follows:

$$Uncertainty = (CI_{upper} - CI_{lower}) / SOC_{mean} \quad (4)$$

where CI_{upper} and CI_{lower} present the upper and lower 95% confident limits of each pixel, and SOC_{mean} is the average SOC value of the performed bootstrap models.

We took 50 bootstrap samples of SOC and associated predictors to implement the RF model. For each time, 10% of the data were selected randomly as independent validation and 90% were used as calibration.

The following indices were calculated: the mean error (ME), the root mean square error (RMSE), and Lin's concordance correlation coefficient (LCCC) (Lin, 1989). They were used as assessment statistics for both calibration and validation, as follows:

$$ME = \frac{1}{N} \sum_{i=1}^N (\hat{y}_i - y_i) \quad (5)$$

$$RMSE = \sqrt{\frac{1}{N} \sum_{i=1}^N (\hat{y}_i - y_i)^2} \quad (6)$$

$$LCCC = \frac{2rs_y s_y}{s_y^2 + s_{\hat{y}}^2 + (\bar{y} - \bar{\hat{y}})^2} \quad (7)$$

In these equations, y and \hat{y} are the observed and predicted values of y , \bar{y} and $\bar{\hat{y}}$ is the mean of the observed and predicted y , s_y^2 and $s_{\hat{y}}^2$ are the variances of the observed and predicted y , r is the Pearson correlation coefficient between the observed and predicted values, and N is the number of comparisons.

2.5. Calculation of soil organic carbon stock

The stock of organic carbon in the 0–20 cm topsoil was calculated as follows:

$$SOC_{stock} = \sum_{i=1}^n T_i \times \rho_i \times SOC_i \times (1 - C_i) \times A_i / 10 \quad (8)$$

where T_i , ρ_i , SOC_i and C_i represent thickness (cm), bulk density ($g\ cm^{-3}$), SOC concentration, and percentage of the fraction $>2\ mm$ of pixel i , respectively. A_i refers to the map resolution (1 km). As we lack the measured bulk density (BD) for each sample, we used pedotransfer functions (PTF) to estimate the BD. We selected six common pedotransfer functions (Table S1) from previous research and the final result was mean of the six estimated values with different

PTFs (Alexander, 1980; Huntington et al., 1989; Manrique and Jones, 1991; Wu et al., 2003; Song et al., 2005; Yang et al., 2007).

2.6. Variation partitioning analysis

To examine the contribution of climate change on SOC dynamic, we collected the meteorological stations data (<http://cdc.cma.gov.cn/>) and calculated the change of temperature and precipitation with the difference of averaged mean annual temperature/precipitation between 2003 and 2006 and averaged mean annual temperature/precipitation between 1984 and 1987. The station data was interpolated into the gridded data by inverse distance weighted method. A redundancy analysis contributed by the package of vegan (Oksanen et al., 2016) in R language (R Core Team, 2013) was used to partition the contribution of land use and climate change to SOC change.

3. Results

3.1. SOC concentrations

The overall mean SOC concentration of the samples in 2004 was 12.5 g kg^{-1} which was slightly higher than the SOC concentrations in 1985 (10.0 g kg^{-1}) (Table 2). Most of the soil samples were collected in cropland (Table 2). In 1985, the soils of the cropland contained the lowest SOC (8.3 g kg^{-1}) whereas the soils under forest had the highest concentrations (17.1 g kg^{-1}). Soils under grassland, marsh and bare soil had SOC concentrations of about 15.1 g kg^{-1} , 16.0 g kg^{-1} and 10.0 g kg^{-1} , respectively (Table 2). For the samples collected in 2004, the soils of the marsh had the highest SOC concentrations (20.8 g kg^{-1}), following in the grassland (13.3 g kg^{-1}), forest (12.7 g kg^{-1}) and cropland (12.2 g kg^{-1}) (Table 2). Over time, SOC increased in soils under cropland, marsh and bare soil whereas it decreased in the soils under forest and grassland. The soils of 1985 showed higher variation than 2004 by the higher standard deviation. (See Table 3.)

3.2. Spatial models of soil organic carbon

The calibration and independent validation of the prediction models are summarized in Table 4 showing reasonable predict accuracies, with the calibration LCCC of 0.91 (0.90–0.92) for 1985 samples, and 0.97 for 2004. We obtained the independent validation LCCC of 0.65 (0.39–0.90) for 1985 and 0.84 (0.77–0.90) for 2004. The RMSEs in 1985 are higher than 2004 for both calibration and validation. The models for 2004 were more robust than for 1985 as indicated by a lower LCCC and RMSE as the sample density was higher.

Fig. 2 showed the importance of the environmental covariates in the prediction models for 1985 and 2004. Some covariates represented similar importance for the two periods, such as slope, TWI, MBI, temperature, precipitation and land use. The vegetation and climatic factors are important predictors, and in particular temperature, precipitation, NDVI

Table 3

Model accuracy for the prediction of soil organic carbon in 1985 and 2004.

Year		Index	Mean	Minimum	Maximum	SD
1985	Calibration	LCCC	0.91	0.90	0.92	0.01
		RMSE	2.08	1.66	2.54	0.56
	Independent validation	ME	0.05	−0.02	0.10	0.03
		LCCC	0.65	0.39	0.90	0.14
		RMSE	6.37	3.14	13.01	2.45
		ME	0.29	−1.12	1.62	0.88
2004	Calibration	LCCC	0.97	0.97	0.97	0.00
		RMSE	1.68	1.60	1.74	0.03
	Independent validation	ME	0.01	−0.01	0.03	0.01
		LCCC	0.84	0.77	0.90	0.03
		RMSE	3.91	3.12	5.33	0.58
		ME	−0.09	−0.84	0.68	0.38

and VNDVI. The aspect, curvature and MBI contribute little to the SOC predictions in 2004 and aspect is the least important factor for the both periods. The PCAs from the spectra of the 2004 soil samples showed high importance in the prediction model. The importance decreases from PC1 to PC3 (Fig. 2).

3.3. Spatial variation of soil C for the 1985 and 2004

The predictions of SOC concentration in the 0–20 cm topsoil for 1985 and 2004 are shown in Fig. 3. SOC concentration in 1985 increased from south to north in the study area. In the south part, the concentration of SOC is mostly under 8 g kg^{-1} . In the middle, which has a higher elevation (Fig. 1), the SOC concentration was higher than in the southern part. In the north, the SOC concentration increased significantly with latitude. The spatial distribution for SOC was similar for both periods (Fig. 3). In the southern half, SOC concentrations were between 8 and 10 g C kg^{-1} , which was higher than in 1985. In the northern part, SOC concentrations increased with latitude.

The uncertainties were different between the two periods because of the difference in the number and location of samples (Fig. 4). The lowest prediction uncertainty was the northern regions. The high uncertainty for the prediction of SOC of 1985 was in the middle part of the area and at the margins in the south where elevation is higher (Fig. 4). The high uncertainty of 2004 was in the middle-north part (Fig. 4) where sample density was lower (Fig. 1).

3.4. Change of soil organic carbon

Between 1985 and 2004, the average SOC concentration decreased under all land use except cropland. The SOC concentration increased by 0.5 g kg^{-1} between 1985 and 2004 in cropland which is the largest land use class in the study area (Table 4). The largest reduction in SOC was in the forest soils with a reduction of 8.8 g kg^{-1} (−38%). The SOC concentrations in grassland had decreased by −21% (Table 4).

Significant changes in SOC concentration were found, and the reduction of SOC was higher in areas with an initial higher concentration

Table 2

Summary statistics of the soil organic carbon concentration (0–20 cm depth) for each land use in 1985 and 2004.

Land use	Number of samples		Mean		Max		Min		SD		Skewness	
	1985	2004	g kg^{-1}		g kg^{-1}		g kg^{-1}		1985	2004	1985	2004
Year	1985	2004	1985	2004	1985	2004	1985	2004	1985	2004	1985	2004
Cropland	446	882	8.3**	12.2**	43.8	43.3	0.8	3	6.9	4.5	1.8	1.4
Forest	58	74	17.1*	12.7*	105.3	48.3	2.5	2.9	17.1	6.2	1.5	1.2
Grassland	51	46	15.1*	13.3*	69.1	31.4	1.1	2.3	10.2	5.1	1.6	0.5
Marsh	16	35	16.0	20.8	39.6	54.9	3.5	2.8	11.6	8.3	0.8	0.2
Bare soil	14	25	10.0	11.1	27.8	26.9	3.6	2.5	7.1	7.2	1.2	0.6
Total	585	1062	10.0**	12.5**	105.3	54.9	0.8	2.3	15.7	6.1	3.6	1.1

Significance code: ** < 0.01, and * < 0.05. SD: standard deviation.

Table 4
Soil carbon change for each land use between 1985 and 2004.

Land use	Soil C change (g kg^{-1})	Rate of change (%)	Area (km^2)
Cropland	0.5	5	374,180
Forest	-8.8	-38	78,713
Grassland	-2.8	-21	60,270
Marsh	-1.3	-7	4057
Bare soil	-1.2	-11	16,102

(Fig. 3). The decrease of SOC mostly occurred in the northern part of the study area (Northeast China). The decrease is over 6 g kg^{-1} . In contrast, SOC increased in the southern part (North China) where the initial SOC is relatively low.

The total stock of soil organic carbon in 1985 and 2004 remains, with the stock 1.68 Pg and 1.66 Pg respectively. We focused on three main land use type in North and Northeast China and analyzed the SOC stock and its change from 1985 to 2004. Generally, cropland contains the largest account of organic carbon. The organic carbon in forest and grassland is much less than in cropland (Fig. S1). About 25% of the SOC was lost during the twenty years under forest soils (Table 5), but 9% of the organic carbon increased in the soils under agricultural crops. Soils under grassland increased by 0.013 Pg SOC with the rate of 25% (Table 5).

Table 5
Soil organic carbon stocks (Pg) and change by land use for 1985 and 2004.

SOC stock	1985 (Pg)	2004 (Pg)	Change (Pg)	Rate of change (%)
Cropland	0.943	1.032	0.094	+9
Forest	0.305	0.227	-0.089	-25
Grassland	0.150	0.113	-0.037	-25

3.5. Effect of land use and climate change on SOC change

Land use contributed more than temperature and precipitation change to SOC change in North and Northeast China (Fig. 5). Across the whole area, land use contributed 38% of the total variation of SOC change while temperature change shared approximate 9% and precipitation change only 5%. Land use accounted for more variation in Northeast China (42%) compared with that in North China (33%) (Fig. 5). Change of temperature showed no significant impact on SOC across the whole study area, as well as in Northeast China and North China specifically. The change of precipitation had a small amount (17%) of impact for the dynamic of SOC in North China but little in Northeast China. Temperature showed no significant contribution to SOC changes in Northeast China while accounted 20% in North China. The total contribution of climate change for SOC variation in North China reached 35% compared with 33% caused by land use but they shared 19% interaction for the total variation (Fig. 5).

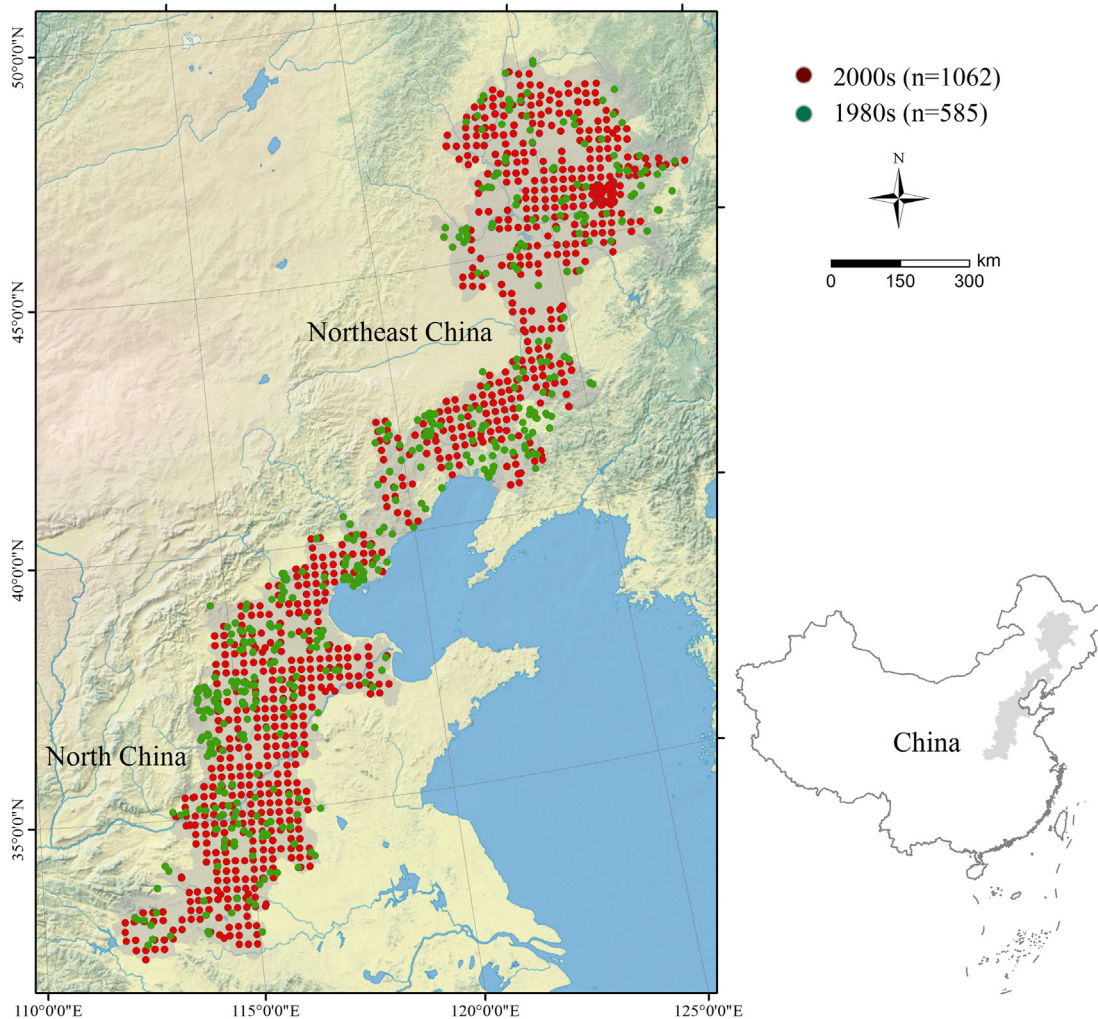


Fig. 1. Study area and sample locations collected in 1980s and 2000s.

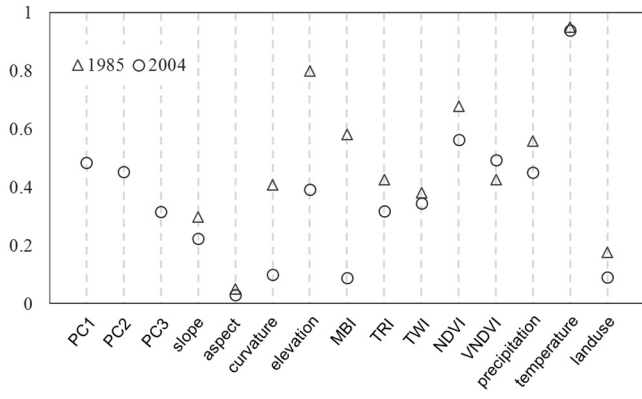


Fig. 2. Covariate importance in the random forest models for the prediction of soil organic carbon concentrations in 1985 and 2004.

4. Discussion

4.1. Digital SOC mapping and its uncertainty

We investigated soil carbon changes in North and Northeast China by mapping SOC concentration in 1985 and 2004. The indices of the prediction accuracy (LCCC of 0.65 for 1985 and 0.84 for 2004) were comparable with other regional studies. For example, Yang et al. (2016) reported LCCC of 0.54 (0.53–0.55) in China and Viscarra Rossel et al. (2014) reported LCCC of 0.81 in Australia. Our result indicated that the soil carbon map for the two periods is reasonable and the comparison between the periods is valid.

The prediction accuracy is different for the two periods and some uncertainties remain in the process. The first uncertainties originate from the spatial variation models and the covariates used. There were 1062 samples in 2004 compared to 585 samples collected from the National Soil Survey collected in the 1980s. More samples were used for calibration in the models of 2004 and better relationship between SOC and environmental was obtained. The samples collected in 2004 were evenly distributed with 30km grids while the samples from the National Soil Survey were not evenly distributed. This affected the model performance as some area may have little data to extract the soil-environment relationship. The environmental covariates and their resolution differed for the two periods. For 2004, soil spectra were used as covariates in the prediction of soil carbon and such data was not available for 1985. The

spectra showed significant impact in the models (Fig. 2) and improved the prediction. Lastly, the NDVI and VNDVI obtained from MODIS data has a higher resolution than the GIMMS that was used for 1985.

Besides the samples and covariates, another uncertainty source is the bulk density, which was themselves predicted by the PTFs rather than measured, was used in calculation of C stock. Therefore uncertainties in the predictions were propagated to the predictions of the SOC stocks. It has been noticed that such inaccuracy in data on bulk density is one of the major sources of uncertainty in the estimation of carbon stocks in soil (Schrumpf et al., 2011). The integration of different PTFs may reduce the uncertainty (Xu et al., 2015). In our study different estimations of organic carbon in soils were found using the disparate PTFs, but the trend of the SOC stock change remains similar for each PTF (Fig. S1). Evidently, to obtain accurate estimates of the SOC stock, measured bulk density is needed, or predict bulk density by combination of various PFT.

4.2. Soil carbon change under different land use

There have been a considerable number of studies on the dynamics of SOC concentration and its stock across the world (Guo and Gifford, 2002; Poeplau et al., 2011; Yu et al., 2012; Xiong et al., 2014; Smith et al., 2016). Our study found small changes in SOC stock across the study area which is the result of increasing soil carbon in cropland and a decrease in the soils under forest and grassland. Similar results have been reported (Xu et al., 2010; Deng et al., 2014; Han et al., 2018). SOC concentration increases in soils under agriculture during the last decades in China (Sun et al., 2010; Yu et al., 2012). Huang and Sun (2006) found that the increase of SOC concentration is from 0.46 g kg⁻¹ to 3.31 g kg⁻¹ for North China and 0.29 g kg⁻¹ to 6.09 g kg⁻¹ for Northeast China in two decades. The main reason for the increase of SOC is the addition of crop residues and organic manure and higher fertilizer application and improved fertilization (Huang and Sun, 2006). In the early 1980s, an increasing amount of fertilizer and levels increased from 120 kg ha⁻¹ in 1980 to 590 kg ha⁻¹ in 2008 (Xu et al., 2006; Shi et al., 2013). These agricultural managements resulted in SOC accumulation (Han et al., 2018).

In our study, SOC was declining in some areas whereas it increased in others (Fig. 3). This was largely dependent on the land use and climatic factors. Large area of land was converted from natural vegetation to cropland in the northeastern part (Fig. S2) which resulted in a carbon loss. The SOC in Northeast China was reported increased during last three decades by Ou et al. (2017). The area with increasing SOC may

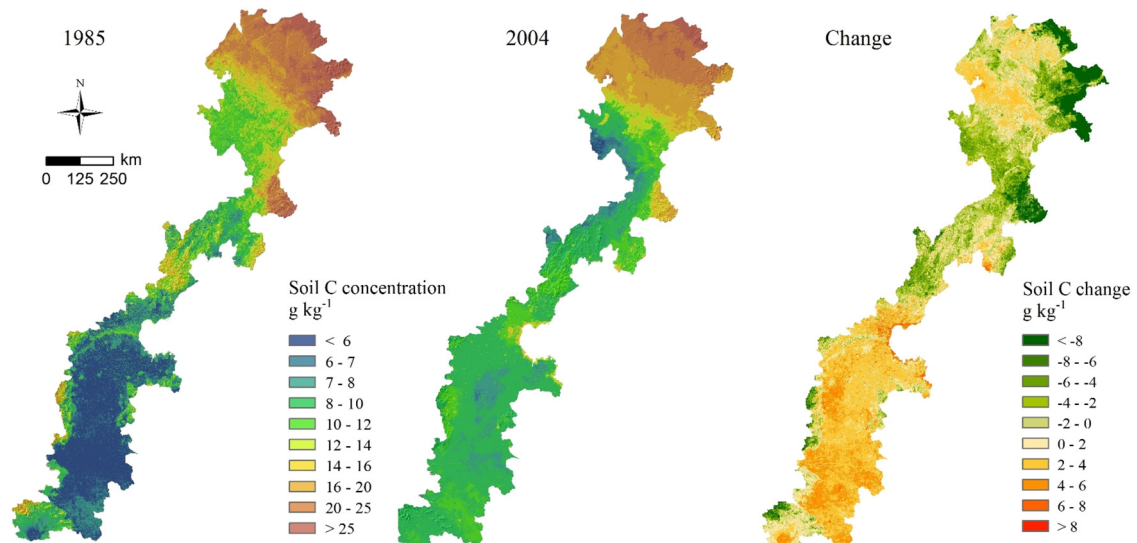


Fig. 3. Soil organic carbon concentrations in 1985 and 2004, and the change over the same period.

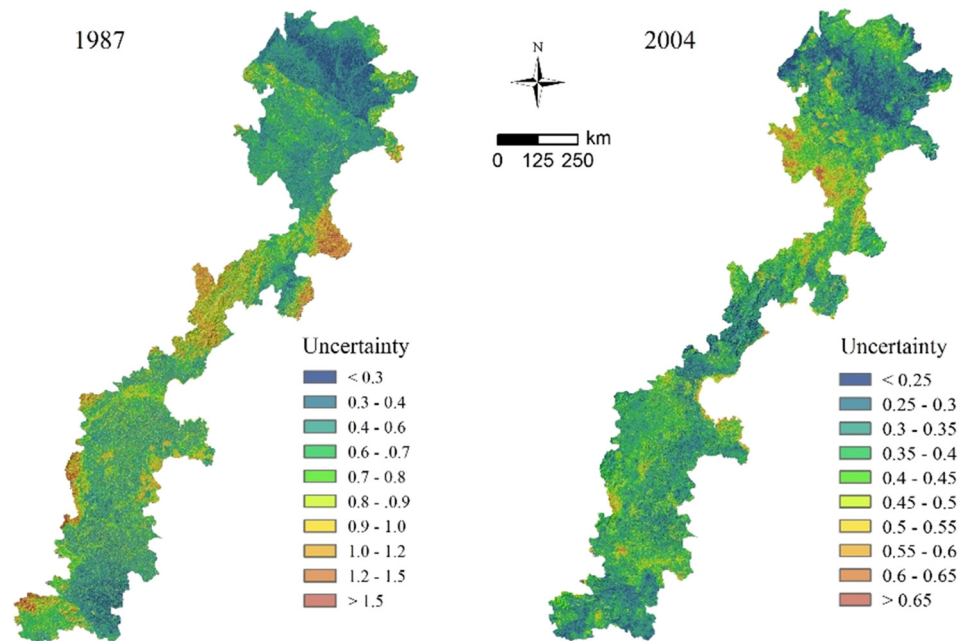


Fig. 4. Uncertainty in the prediction model of soil organic carbon concentrations (g kg⁻¹) for 1985 and 2004.

be partially cropland with a long history of cultivation and addition of fertilizers and crop residues. Afforestation and paddy land use have considerable potential in restoring the carbon into soil (Wu et al., 2003).

4.3. Influence of land use and climate change on soil carbon stock

Many studies have reported that climate change was an important determinant of SOC concentration (Ou et al., 2017). The positive impact of temperature on SOC decomposition was revealed by various studies (Kirschbaum, 1995). However, the feedback of SOC to global warming is still a concern due to the complex reaction of ecosystems to the climate change. The increasing temperature and precipitation may lead to higher decomposition of SOC. It may also increase the SOC due to vegetation-derived carbon inputs (Davidson and Janssens, 2006). The feedback of SOC to global warming in temperate zone is regarded with great potential of decline in concentration (Piao et al., 2009; Wiesmeier et al., 2016). In our study, large SOC loss was found in Northeast China's forests but less change in cropland while SOC increased in North China under similar climate change condition. The change of SOC showed significant difference under different land use rather than following the trend of temperature and precipitation change. The variation analysis revealed that land use is the dominant

driver of SOC change across the whole study area. However the effects of land use and climate change are different in North China and Northeast China. The difference may due to the land use and land use conversion. The North China remains cropland from 1980s to 2000s while large area was converted from forest and grassland to cropland in Northeast China (Fig. S2).

Land use conversion affects SOC stocks (Deng et al., 2016). Our study found soil carbon accumulation in North China and loss of soil carbon in Northeast China (Fig. 3). Lands of forest and grassland have been converted to cropland during the 1980s to 2000s (Fig. S2). Intensive conversion of land use appears in northeast compared with north China. As a result, the average thickness of soils has decreased 20–30 cm in some area in Northeast due to soil erosion (Xu et al., 2010). The loss of SOC in land is related to the conversion of other native forest and grassland to cropland (Fig. 3, Fig. S2). Global analysis found SOC loss after deforestation between 30% and 42% and conversion from grassland to cropland caused decline of 24–59% of total SOC (Guo and Gifford, 2002; Van Wesemael et al., 2010; Wang et al., 2011). As SOC loss happen rapidly in the earlier stage after natural soils were converted, soil carbon is more potentially losing carbon where lands were reclaimed with a shorter history. Unlike North China plain with a long history of agriculture production, Northeast

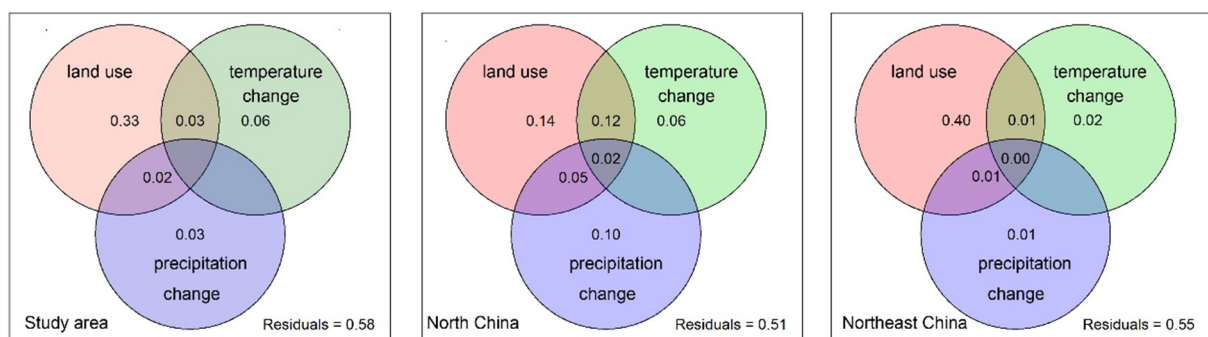


Fig. 5. Variation contribution to the soil organic carbon change by the land use and climate change using variation partitioning analysis in the whole study, North China and Northeast China, respectively.

China shared a shorter history of anthropogenic cultivation (Yu et al., 2006). In contrast, the soil in Northeast China contains high original organic carbon but decrease significantly during the 1980s to 2000s. The reason that Northeast China is a net source of greenhouse gas to the atmosphere owing to overharvesting and degradation of forests in recent years.

Anthropogenic activities influence SOC concentrations but also impacts spatial heterogeneity of SOC. The decline of concentration in soil with higher carbon and the increase in soil with lower carbon makes the range of SOC concentration in 2004 is smaller than that in 1985 (Table 2). In North China, SOC showed more homogeneous variation in 2004 than 1985. The management of land use can have high influence on the dynamics of SOC. Although magnificent loss of carbon in Northeast China soil, but the general soil carbon stock during the two decades remains. Soil has high potential on sink greenhouse gas in cropland and to reduce emission of C, forests should be preserved and overharvesting should be avoided.

5. Conclusions

Our study estimated the 0–20 cm topsoil organic carbon concentration and stock change between 1985 and 2004. The digital soil mapping approach predicted the spatial variation of SOC for the two periods using environmental covariates in a random forest model. The following conclusions can be made:

- i. Random forest is efficient on prediction of SOC spatial variation at large scale. SOC concentration shared a similar trend for the two periods, with lower SOC in Northeast China and higher in North China Plain. Soil carbon increase in the northern part whereas it decreased in most northeast areas.
- ii. The overall stock of SOC was stable. Carbon stock increased 0.094 Pg in the soils of cropland with a rate of 9%. Significant carbon loss occurred in soils under forest (−25%) and grassland (−25%).
- iii. Land use change is the predominant driver of SOC changes in North and Northeast China. Climate change accounted similar contribution for SOC change compared to land use change while less contribution in Northeast China.

This study revealed that land use change had significant effect on soil organic carbon. Our results point out the emission of greenhouse under inappropriate land use change and proved that cropland had high potential on carbon sequestration.

Acknowledgements

This study was undertaken while the first authors was a visiting student at UW Madison. The research was supported by National Key Research and Development Program of China (2017YFD0700501) and Research Fund of State Key Laboratory of Soil and Sustainable Agriculture, Nanjing Institute of Soil Science, Chinese Academy of Science (Y412201430).

Appendix A. Supplementary data

Supplementary data to this article can be found online at <https://doi.org/10.1016/j.scitotenv.2018.08.016>.

References

Alexander, E.B., 1980. Bulk densities of California soils in relation to other soil properties 1. *Soil Sci. Soc. Am. J.* 44 (4), 689–692.
 Bishop, T.F.A., McBratney, A.B., Laslett, G.M., 1999. Modelling soil attribute depth functions with equal-area quadratic smoothing splines. *Geoderma* 91 (1), 27–45.
 Breiman, L., 2001. Random forests. *Mach. Learn.* 45, 5–32.

Chen, S., Martin, M.P., Saby, N.P., et al., 2018. Fine resolution map of top-and subsoil carbon sequestration potential in France. *Sci. Total Environ.* 630, 389–400.
 Costa Junior, C., Corbeels, M., Bernoux, M., et al., 2013. Assessing soil carbon storage rates under no-tillage: comparing the synchronic and diachronic approaches. *Soil Tillage Res.* 134, 207–212.
 Davidson, E.A., Janssens, I.A., 2006. Temperature sensitivity of soil carbon decomposition and feedbacks to climate change. *Nature* 440 (7081), 165.
 Deng, L., Liu, G.B., Shangguan, Z.P., 2014. Land-use conversion and changing soil carbon stocks in China's 'Grain-for-Green' Program: a synthesis. *Glob. Chang. Biol.* 20 (11), 3544–3556.
 Deng, L., Zhu, G.Y., Tang, Z.S., et al., 2016. Global patterns of the effects of land-use changes on soil carbon stocks. *Glob. Ecol. Conserv.* 5, 127–138.
 Don, A., Schumacher, J., Freibauer, A., 2011. Impact of tropical land-use change on soil organic carbon stocks—a meta-analysis. *Glob. Chang. Biol.* 17 (4), 1658–1670.
 Falloon, P., Smith, P., 2002. Simulating SOC changes in long-term experiments with RothC and CENTURY: model evaluation for a regional scale application. *Soil Use Manag.* 18 (2), 101–111.
 Grinand, C., Le Maire, G., Vieilledent, G., et al., 2017. Estimating temporal changes in soil carbon stocks at ecoregional scale in Madagascar using remote-sensing. *Int. J. Appl. Earth Obs. Geoinf.* 54, 1–14.
 Guo, L.B., Gifford, R.M., 2002. Soil carbon stocks and land use change: a meta-analysis. *Glob. Chang. Biol.* 8 (4), 345–360.
 Han, D., Wiesmeier, M., Conant, R.T., et al., 2018. Large soil organic carbon increase due to improved agronomic management in the North China Plain from 1980s to 2010s. *Glob. Chang. Biol.* 24 (3), 987–1000.
 Huang, Y., Sun, W., 2006. Changes in topsoil organic carbon of croplands in mainland China over the last two decades. *Chin. Sci. Bull.* 51 (15), 1785–1803.
 Huntington, T.G., Johnson, C.E., Johnson, A.H., et al., 1989. Carbon, organic matter, and bulk density relationships in a forested spodosol. *Soil Sci.* 148 (5), 380–386.
 IPCC, 2013. Summary for policy makers. In: Stocker, T., Qin, D., Plattner, G., Tignor, M., Allen, S., Boschung, J., Nauels, A., Xia, Y., Bex, V., Midgley, P. (Eds.), *Climate Change 2013: The Physical Science Basis. Contribution of Working Group I to the Fifth Assessment Report of the Intergovernmental Panel on Climate Change*. Cambridge University Press, Cambridge, United Kingdom and New York, NY, USA, pp. 1–30.
 Kirschbaum, M.U., 1995. The temperature dependence of soil organic matter decomposition and the effect of global warming on soil organic C storage. *Soil Biol. Biochem.* 27 (6), 753–760.
 Lin, L., 1989. A concordance correlation coefficient to evaluate reproducibility. *Biometrics* 45, 255–268.
 Liu, J., Kuang, W., Zhang, Z., 2014. Spatiotemporal characteristics, patterns, and causes of land-use changes in China since the late 1980s. *J. Geogr. Sci.* 24 (2), 195–210.
 Ma, Z., Shi, Z., Zhou, Y., et al., 2017. A spatial data mining algorithm for downscaling TMPA 3B43 V7 data over the Qinghai–Tibet Plateau with the effects of systematic anomalies removed. *Remote Sens. Environ.* 200, 378–395.
 Manrique, L.A., Jones, C.A., 1991. Bulk density of soils in relation to soil physical and chemical properties. *Soil Sci. Soc. Am. J.* 55 (2), 476–481.
 McBratney, A.B., Santos, M.M., Minasny, B., 2003. On digital soil mapping. *Geoderma* 117 (1), 3–52.
 Nadeu, E., Gobin, A., Fiener, P., et al., 2015. Modelling the impact of agricultural management on soil carbon stocks at the regional scale: the role of lateral fluxes. *Glob. Chang. Biol.* 21 (8), 3181–3192.
 NASA Land Processes Distributed Active Archive Center (LP DAAC), 2001. MODIS Land Products. USGS/Earth Resources Observation and Science (EROS) Center, Sioux Falls, South Dakota.
 Oksanen, J., Blanchet, G., Kindt, Roeland, et al., 2016. *vegan: community ecology package*. R package version 2. <http://CRAN.R-project.org/package=vegan> (3–5).
 Ou, Y., Rousseau, A.N., Wang, L., et al., 2017. Spatio-temporal patterns of soil organic carbon and pH in relation to environmental factors—a case study of the Black Soil Region of Northeastern China. *Agric. Ecosyst. Environ.* 245, 22–31.
 Piao, S., Fang, J., Ciais, P., et al., 2009. The carbon balance of terrestrial ecosystems in China. *Nature* 458 (7241), 1009.
 Poepplau, C., Don, A., Vesterdal, L., et al., 2011. Temporal dynamics of soil organic carbon after land-use change in the temperate zone—carbon response functions as a model approach. *Glob. Chang. Biol.* 17 (7), 2415–2427.
 R Core Team, 2013. *R: A Language and Environment for Statistical Computing*. R Foundation for Statistical Computing, Vienna, Austria.
 Sanchez, P.A., Ahamed, S., Carré, F., et al., 2009. Digital soil map of the world. *Science* 325 (5941), 680–681.
 Schrumppf, M., Schulze, E.D., Kaiser, K., Schumacher, J., 2011. How accurately can soil organic carbon stocks and stock changes be quantified by soil inventories? *Biogeosciences* 8, 723–769.
 Shi, X.Z., Yu, D.S., Warner, E.D., et al., 2004. Soil database of 1:1,000,000 digital soil survey and reference system of the Chinese genetic soil classification system. *Soil Surv. Horiz.* 45 (4), 129–136.
 Shi, W., Tao, F., Liu, J., 2013. Changes in quantity and quality of cropland and the implications for grain production in the Huang-Huai-Hai Plain of China. *Food Sec.* 5 (1), 69–82.
 Shi, Z., Ji, W., Viscarra Rossel, R.A., et al., 2015. Prediction of soil organic matter using a spatially constrained local partial least squares regression and the Chinese vis-NIR spectral library. *Eur. J. Soil Sci.* 66, 679–687.
 Smith, P., House, J.I., Bustamante, M., et al., 2016. Global change pressures on soils from land use and management. *Glob. Chang. Biol.* 22 (3), 1008–1028.
 Song, G., Li, L., Pan, G., Zhang, Q., 2005. Topsoil organic carbon storage of China and its loss by cultivation. *Biogeochemistry* 74 (1), 47–62.
 Stow, D.A., Hope, A., McGuire, D., et al., 2004. Remote sensing of vegetation and land-cover change in Arctic Tundra Ecosystems. *Remote Sens. Environ.* 89 (3), 281–308.

- Sun, W., Huang, Y., Zhang, W., et al., 2010. Carbon sequestration and its potential in agricultural soils of China. *Glob. Biogeochem. Cycles* 24 (3), GB2001.
- Tucker, C.J., Pinzon, J.E., Brown, M.E., 2004. *Global Inventory Modeling and Mapping Studies*, NA94apr15b.n11-V1g, 2.0. Global Land Cover Facility, University of Maryland, College Park, Maryland (1994).
- USGS, 2006. Shuttle Radar Topography Mission, 1 Arc Second scenes. Global Land Cover Facility - University of Maryland, Maryland, US.
- Van Wesemael, B., Paustian, K., Meersmans, J., et al., 2010. Agricultural management explains historic changes in regional soil carbon stocks. *Proc. Natl. Acad. Sci.* 107 (33), 14926–14930.
- Viscarra Rossel, R.A., Webster, R., Bui, E.N., et al., 2014. Baseline map of organic carbon in Australian soil to support national carbon accounting and monitoring under climate change. *Glob. Chang. Biol.* 20 (9), 2953–2970.
- Wang, S., Wilkes, A., Zhang, Z., et al., 2011. Management and land use change effects on soil carbon in northern China's grasslands: a synthesis. *Agric. Ecosyst. Environ.* 142 (3), 329–340.
- Wiesmeier, M., Poeplau, C., Sierra, C.A., et al., 2016. Projected loss of soil organic carbon in temperate agricultural soils in the 21st century: effects of climate change and carbon input trends. *Sci. Rep.* 6, 32525.
- Wu, H., Guo, Z., Peng, C., 2003. Land use induced changes of organic carbon storage in soils of China. *Glob. Chang. Biol.* 9 (3), 305–315.
- Xiong, X., Grunwald, S., Myers, D.B., et al., 2014. Interaction effects of climate and land use/land cover change on soil organic carbon sequestration. *Sci. Total Environ.* 493, 974–982.
- Xu, Y., Zhang, F.R., Zheng, B.Z., et al., 2006. Influence of economic development level on topsoil organic carbon over time. *Ecol. Environ.* 15, 74–79 (in Chinese with English abstract).
- Xu, X.Z., Xu, Y., Chen, S.C., et al., 2010. Soil loss and conservation in the black soil region of Northeast China: a retrospective study. *Environ. Sci. Pol.* 13 (8), 793–800.
- Xu, L., He, N.P., Yu, G.R., et al., 2015. Differences in pedotransfer functions of bulk density lead to high uncertainty in soil organic carbon estimation at regional scales: evidence from Chinese terrestrial ecosystems. *J. Geophys. Res. Biogeosci.* 120 (8), 1567–1575.
- Yang, Y., Mohammad, A., Feng, J., et al., 2007. Storage, patterns and environmental controls of soil organic carbon in China. *Biogeochemistry* 84 (2), 131–141.
- Yang, R.M., Zhang, G.L., Yang, F., et al., 2016. Precise estimation of soil organic carbon stocks in the northeast Tibetan Plateau. *Sci. Rep.* 6, 21842.
- Ye, Y., Fang, X., Ren, Y., et al., 2009. Cropland cover change in Northeast China during the past 300 years. *Sci. China Ser. D Earth Sci.* 52 (8), 1172–1182.
- Yu, G., Fang, H., Gao, L., et al., 2006. Soil organic carbon budget and fertility variation of black soils in Northeast China. *Ecol. Res.* 21 (6), 855–867.
- Yu, Y., Huang, Y., Zhang, W., 2012. Modeling soil organic carbon change in croplands of China, 1980–2009. *Glob. Planet. Chang.* 82, 115–128.
- Zhou, Y., Biswas, A., Ma, Z., et al., 2016. Revealing the scale-specific controls of soil organic matter at large scale in Northeast and North China Plain. *Geoderma* 271, 71–79.